

# Optimized Fixed-Time Synergetic Controller via a modified Salp Swarm Algorithm for Acute and Chronic HBV Transmission System

Saadi Achour<sup>1,✉</sup>, Khalil Mokhtari<sup>2</sup>, Abdelaziz Rahmoune<sup>1</sup>, Fares Yazid<sup>1</sup>

<sup>1</sup>Laboratory of Pure and Applied Mathematics, University Amar Telidji of Laghouat, BP 37G, Ghardaia Road, 03000 Laghouat, Algeria

<sup>2</sup>Department of Industrial Engineering, University Abbes Laghrour of Khenchela, BP 1252, Route de Batna, Khenchela 40004, Algeria

saadi.achour@lagh-univ.dz✉, khalil.mokhtari@univ-khenchela.dz, a.rahmoune@lagh-univ.dz, f.yazid@lagh-univ.dz

## Abstract

*In this report, we propose a Salp Swarm Algorithm (SSA) optimized Fixed-Time Synergetic Control (FTSC) strategy to develop a possible infection spread control approach. The utilization of the SSA optimization algorithm for optimizing the Synergetic Control (SC) fraction parameters presents a non-trivial challenge due to the restriction that only odd numbers can be used for the fractional power. Therefore, an enhanced and adapted version of the SSA algorithm is proposed to effectively address this specific scenario. Our strategic approach centers on the reduction of the numbers of susceptible, acutely infected, and chronically infected individuals by employing control parameters such as isolation, treatment, and vaccination. The objective is to drive these target state variables to their smallest values in a fixed-time, thereby effectively controlling the spread of the virus. We support our proposal with numerical simulations to demonstrate the feasibility and effectiveness of the control strategy. A comparison is conducted between FTSC and SC in scenarios with and without optimization. The results indicated that FTSC holds a distinct advantage, consistently demonstrating significant progress, with up to 30% reduction in the total convergence time to zero, outperforming SC in each case.*

**Keywords:** Salp Swarm Optimization Algorithm, Synergetic Controller, Fixed-time Control, Lyapunov Stability, Hepatitis B Virus, Epidemic System.

Received: 19 September 2023

Accepted: 30 October 2023

Online: 05 November 2023

Published: 20 December 2023

## 1 Introduction

Hepatitis B Virus (HBV) belongs to the Hepadnaviridae family, as documented by Magnius et al. [25]. Upon entering the body, HBV targets hepatocytes, the liver cells [35]. Consequently, the immune system responds by initiating inflammation in the liver [4]. The infection of HBV progresses through two distinct phases: acute hepatitis and chronic hepatitis [6]. During the initial six months, known as the acute hepatitis B period, the immune system typically succeeds in clearing the virus from the body, resulting in complete recovery within a few months. However, if HBV persists in the body and leads to significant health complications, it transitions into chronic hepatitis B. Despite the absence of prior severe illness, chronic hepatitis B can result in liver scarring, potentially leading to liver failure and even liver cancer [21, 32].

The transmission of this critical disease, occurs through the exchange of bodily fluids in humans. Initially, a viral infection manifests as a severe phase within the individual's body, which can potentially evolve into a chronic condition. Prolonged exposure to the virus increases the risk of developing cirrhosis and liver cancer [23]. The HBV poses a significant

threat and raises serious concerns due to its potential to cause a fatal illness [6]. In 2015 alone, a staggering 887,000 individuals worldwide lost their lives to this virus, which has been detected in approximately 257 million people [3]. According to the World Health Organization (WHO), Hepatitis B presents a significant global health challenge, with its highest prevalence observed in the WHO Western Pacific Region and the WHO African Region, affecting approximately 116 million and 81 million individuals, respectively, as chronic carriers. In the WHO Eastern Mediterranean Region, around 60 million people are infected, while the WHO South-East Asia Region has an estimated 18 million cases. Additionally, the WHO European Region accounts for approximately 14 million infections, and the WHO Region of the Americas reports 5 million cases of chronic hepatitis B. However, it is crucial to note that vaccination against HBV has proven to be an effective preventive measure against infection.

Within the realm of real-world phenomena, mathematical modeling emerges as a potent tool for effectively delineating the intricate dynamics characterizing a wide array of diseases [37, 38, 39, 40, 41]. The establishment of control strategies for hepatitis B epidemic systems can be achieved through the utiliza-

tion of mathematical model as evident in the literature sources [12, 10, 28, 16].

In this article, we investigate the HBV transmission model developed in [16] to design an optimized FTSC strategy. The control system implemented in this study to combat the hepatitis B epidemic encompasses a comprehensive and integrated strategy that incorporates various elements such as isolation, vaccination, and treatment to effectively manage the spread of the disease. It leverages the analytical design of aggregated regulators (ADAR) method that combines the strengths of different control mechanisms to create a synergistic effect, enhancing the overall efficiency and efficacy of the control system [36, 5]. By integrating isolation measures, which involve isolating infected individuals to prevent transmission, with widespread vaccination programs and effective treatment protocols, the control system maximizes its impact on reducing the prevalence and consequences of hepatitis B [18].

The ADAR method, in conjunction with the synergetic control theory, as developed and advanced by Kolesnikov et al. [19] and Nusawardhana et [29], brings about several advantageous features for the control systems. These features include:

- Global stability,
- Improved coordination and interaction between the different control inputs,
- Enhanced adaptability to changing conditions and dynamics of the epidemic,
- The ability to tailor the control measures based on specific characteristics of the affected population.

The literature [11, 24, 33, 14, 17] showcases multiple instances of synergetic control applications within the engineering domain.

In contrast to the previous studies, the proposed control approach enables the control system designers to effectively address the challenges posed by the HBV infection. By harnessing the power of synergistic interactions between isolation, vaccination, and treatment strategies, the control system becomes more robust, responsive, and capable of mitigating the impact of the disease in a *fixed-time*. Therefore, attaining these characteristics relies on the selection of appropriate macrovariables and controller parameters by the designer [31].

The SSA is a metaheuristic optimization algorithm proposed in [27]. This class of algorithms has proven its effectiveness, as they have been extensively used to solve real-world problems [13, 1, 26]. However, SSA has some limitations, such as a slow convergence rate, poor population diversity, and exploration issues [9, 22, 8, 7]. To address these vulnerabilities, new versions of SSA have emerged, such as the Amended Salp Swarm Optimizer (ASSO) [9] and the Quadratic Approximation Salp Swarm Algorithm (QA-SSA) [34]. We chose to use the classical SSA because the mentioned drawbacks

mostly occur in high-dimensional scenarios with numerous constraints, which is not our case.

Our study introduces and modifies the SSA optimization method to effectively determine optimal values for the parameters of the FTSC, particularly those associated with fractional power. This modification is imperative because of the inability of the basic SSA algorithm to directly optimize the fractional parameters of the FTSC. Notably, to maintain stability in the closed-loop system using the Lyapunov direct method, the fractional parameters of the FTSC must be odd numbers, which poses a non-trivial challenge for the SSA. To tackle this challenge, we propose a modified version of the SSA algorithm that extends its applicability to Fixed Time Controllers, marking the first instance of such an adaptation. The contributions of the present paper are summarized in what follows:

- Proposition of an SSA *optimized* FTSC strategy for the spread of hepatitis B infection,
- Proposition of a *projection method* for the SSA to approximate the fractional parameters with a high degree of precision, effectively converting them into odd feasible numbers, ensuring almost exact slaps approximation,
- The stability analysis of the optimized closed-loop system is formally established via Lyapunov direct method.

## 2 Mathematical Modeling

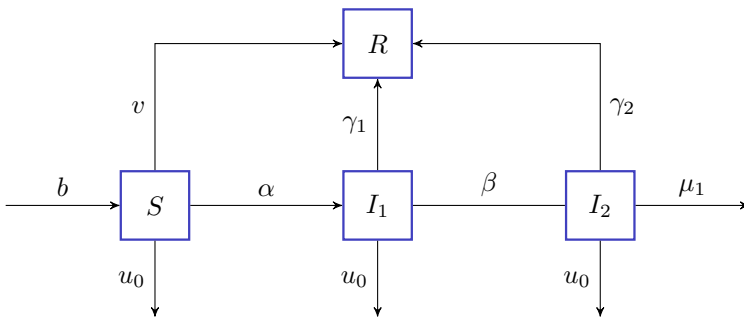
In this section, we introduce the mathematical model concerning the transmission of HBV that is of our primary interest. This model was initially formulated in [16] and builds upon the earlier work of Khan et al. in 2015 [15]. The model categorizes the host population into four distinct groups:  $S$ ,  $I_1$ ,  $I_2$ , and  $R$ , representing susceptible individuals who are at risk of infection, individuals infected with acute hepatitis, individuals affected by chronic hepatitis, and those who have developed lifelong immunity after recovery from the infection, respectively. The flowchart depicting the dynamics of virus transmission can be observed in Figure 1.

The dynamical model of HBV transmission system is described as:

$$\begin{cases} \frac{dS(t)}{dt} = b - \alpha S(t)I_2(t) - (\mu_0 + v) S(t) \\ \frac{dI_1(t)}{dt} = \alpha S(t)I_2(t) - (\mu_0 + \beta + \gamma_1) I_1(t) \\ \frac{dI_2(t)}{dt} = \beta I_1(t) - (\mu_0 + \mu_1 + \gamma_2) I_2(t) \\ \frac{dR(t)}{dt} = \gamma_1 I_1(t) + \gamma_2 I_2(t) + vS(t) - \mu_0 R(t). \end{cases} \quad (1)$$

With the following initial conditions

$$S(0) \geq 0, \quad I_1(0) \geq 0, \quad I_2(0) \geq 0, \quad R(0) \geq 0.$$



- $b$  Birth rate
- $\alpha$  Moving rate from  $S$  to  $I_1$
- $\beta$  Moving rate from  $I_1$  to  $I_2$
- $\gamma_1$  Recovery rate from  $I_1$  to  $R$
- $\gamma_2$  Recovery rate from  $I_2$  to  $R$
- $\mu_0$  The rate of natural mortality
- $\mu_1$  Mortality rate resulting from HBV
- $v$  The rate of vaccination

Figure 1: HBV transmission diagram.

In order to mitigate the transmission of HBV infection within the community, we employ FTSC to construct a control strategy for HBV transmission. The aim of this research is to reduce the occurrence of HBV infection in the population by increasing the count of recovered individuals  $R(t)$ , while decreasing the number of susceptible individuals  $S(t)$  and individuals afflicted with acute hepatitis B  $I_1(t)$  and chronic hepatitis B  $I_2(t)$ . This is accomplished by employing time-dependent control parameters, which involve isolating both infected and uninfected individuals  $u_1(t)$ , implementing treatment measures  $u_2(t)$ , and administering hepatitis B vaccination interventions  $u_3(t)$ .

The control inputs are defined as:

$$U = \{(u_1, u_2, u_3) \mid u_i(t) \text{ is Lebesgue measurable on } [0, 1], 0 \leq u_i(t) \leq 1, \text{ for } i = 1, 2, 3\}.$$

This constraint imposes a limitation on all controllers, confining their values within the range of 0 to 1 [16]. The system (2) represents the HBV transmission model, which incorporates the control parameters  $u_1$ ,  $u_2$ , and  $u_3$ . These control parameters are essential for implementing FTSC technique to effectively regulate the spread of the HBV infection.

$$\begin{cases} \frac{dS(t)}{dt} = b - \alpha S(t)I_2(t)(1 - u_1(t)) - \mu_0 S(t) - u_3(t)S(t) \\ \frac{dI_1(t)}{dt} = \alpha S(t)I_2(t)(1 - u_1(t)) - (\mu_0 + \beta + \gamma_1)I_1(t) - (u_2(t) + u_3(t))I_1(t) \\ \frac{dI_2(t)}{dt} = \beta I_1(t) - (\mu_0 + \mu_1 + \gamma_2)I_2(t) - (u_2(t) + u_3(t)) \cdot I_2(t) \\ \frac{dR(t)}{dt} = \gamma_1 I_1(t) + \gamma_2 I_2(t) + u_3(t)S(t) - \mu_0 R(t) + (u_2(t) + u_3(t))(I_1(t) + I_2(t)). \end{cases} \quad (2)$$

With the initial conditions

$$S(0) \geq 0, \quad I_1(0) \geq 0, \quad I_2(0) \geq 0, \quad R(0) \geq 0.$$

### 3 A Brief Review of FTSC Theory and SSA Algorithm

#### 3.1 FTSC Theory

The fixed-time synergetic controller is a control strategy that can stabilize a dynamical system in a fixed and pre-specified time, regardless of its initial conditions.

The primary objective of the control approach in this study is to achieve a fixed-time synergetic solution for stabilizing a dynamical system. To this end, we introduce the concept of a fixed-time synergetic controller and present a fundamental lemma that underpins its design.

**Lemma 1.** [2] Given a system of differential equations, where  $Z$  is a function that is positively defined:

$$\begin{cases} \dot{Z} = -\alpha_1 Z^{\zeta_1} - \beta_1 Z^{\zeta_2}, \\ Z(0) = Z_0 \end{cases} \quad (3)$$

where  $\alpha, \beta$  are positive real numbers,  $\zeta_1$  and  $\zeta_2$  are positive numbers that satisfy  $\zeta_1 > 1, 0 < \zeta_2 < 1$ . The convergence time of  $Z$  for stabilizing to the origin is set to be  $T(Z_0)$ , then  $Z$  will converge to the origin within an upper bounded constant fixed-time  $T_{\max}(Z)$ , that is  $\lim_{Z_0 \rightarrow \infty} [T(Z_0)] \leq T_{\max}(Z)$ , and  $T_{\max}(Z) = \frac{1}{\alpha} \frac{1}{(\zeta_1 - 1)} + \frac{1}{\beta} \frac{1}{(1 - \zeta_2)}$ .

The nonlinear system (2) requires the control inputs  $u_1(t), u_2(t)$  and  $u_3(t)$  to be determined through FTSC theory. This approach guarantees that the system dynamics move from any initial state to an invariant manifold and eventually return to the origin of system (2). The control function is based on a specific macrovariable  $\varphi$ , which is a function of the system's state variables. The selection of macrovariables is critical and must be made carefully by the designer. Moreover, the macrovariables must satisfy the following conditions to ensure effective control of the system [19]:

$$T\dot{\varphi} + \theta(\varphi) = 0 \quad (4)$$

where,  $T$  represents a design parameter that characterizes how rapidly the macrovariable  $\varphi$  approaches the invariant manifold, defined by  $\varphi(x, t) = 0$ . Meanwhile,  $\theta(\varphi)$  is a differentiable function of  $\varphi$  that is chosen in a smooth manner, subject to the following conditions [20]:

C1:  $\theta(\varphi)$  invertible and differentiable,

C2:  $\theta(0) = 0$ ,

C3:  $\theta(\varphi)\varphi > 0, \forall \varphi \neq 0$ .

**Lemma 2.** [2] The function  $\theta(\varphi)$  satisfies the previous conditions if it is selected in the following form:

$$\theta(\varphi) = \varphi^{(n/m)} + \varphi^{(m/n)} \quad (5)$$

Thus, according to Lemma 2, the macrovariable dynamics can be written as follows:

$$T\dot{\varphi} + \varphi^{(n/m)} + \varphi^{(m/n)} = 0. \quad (6)$$

By virtue of Lemma 1 and equation (5), the macrovariable  $\varphi$  converges to the invariant manifold  $\varphi(x, t) = 0$  within a fixed time, and remains there indefinitely. The duration of convergence is determined by  $T(\varphi_0)$ , which is bounded above by a constant,  $\lim_{\varphi_0 \rightarrow \infty} [T(\varphi_0)] \leq T_{\max}(\varphi)$ . This is subject to the following condition:

$$T_{\max}(\varphi) = T \frac{(n+m)}{(n-m)}. \quad (7)$$

The values of  $n$ ,  $m$ , and  $T$  are design parameters that need to be *carefully* selected to ensure that the macrovariable converges to the invariant manifold at the desired rate. These parameters are directly related to the self-organizing forces at play in the SC theory. If chosen appropriately, the self-organizing speed required can be achieved.

In our study, the gains  $T$ ,  $n$  and  $m$  of the proposed controller are optimized by using the SSA algorithm that will be presented in the next subsection.

### 3.2 SSA Algorithm

The SSA is a bio-inspired optimization technique specifically tailored for engineering design challenges. It draws its inspiration from the swarming behavior observed in salps as they navigate and feed in aquatic environments [30]. The groundbreaking introduction of this algorithm was pioneered by Mirjalili et al. in their seminal work [27].

Within the mathematical framework of salp chains, the salp population is partitioned into two distinct factions: the leader and the followers. Positioned at the forefront of the chain, the leader guides the collective movement of the swarm, while the followers dutifully trail its path. Operating within an  $n$ -dimensional search space, where  $n$  denotes the number of variables involved in the problem, the positions of the salps are precisely determined. These positional values are recorded in a two-dimensional matrix, designated as ‘ $x$ ’, which comprehensively encapsulates the potential solution locations. The overarching objective of the swarm is to optimize the food source denoted as ‘ $F$ ’ within the confines of the search space [27].

The leader’s position is updated based on the following equation, which governs the dynamic movement of the salp swarm:

$$x_j^1 = \begin{cases} F_j + c_1 ((ub_j - lb_j) c_2 + lb_j) & c_3 \geq 0 \\ F_j - c_1 ((ub_j - lb_j) c_2 + lb_j) & c_3 < 0. \end{cases} \quad (8)$$

The leader’s position, represented as  $x_j^1$ , is determined based on the food source position  $F_j$  in the  $j$ th dimension, with  $lb_j$  and  $ub_j$  specifying the lower and upper bounds of that dimension. Random numbers  $c_1$ ,  $c_2$ , and  $c_3$  are generated from the range of  $[0, 1]$  to contribute to the leader’s position update.

---

#### Algorithm 1 SSA Pseudo-code.

---

- 1: Generate the salp population  $x_i$  ( $i = 1, \dots, k$ ) according to  $lb$  and  $ub$
  - 2: **while** Stop condition is not satisfied **do** ▷  
the fitness function error is negligible between two successive search agents ( $< \epsilon$ )
  - 3:   Compute the fitness for every search agent, which in this context are referred to as “salps”
  - 4:    $F =$  best search agent
  - 5:   Update  $c_1$  by Eq (9)
  - 6:   **for** each salp  $x_i$  **do**
  - 7:     **if**  $i = 1$  **then**
  - 8:       Adjust/Update the location of the primary (leading) salp by Eq (8)
  - 9:     **else**
  - 10:       Adjust/Update the location of the primary (leading) salp by Eq (11)
  - 11:     **end if**
  - 12:   **end for**
  - 13:   Based on the upper and lower boundaries of the variables, amend the salp
  - 14: **end while**
  - 15: return  $F$
- 

In SSA, the coefficient  $c_1$  plays a crucial role as it manages the delicate balance between exploitation and exploration according to the following relation:

$$c_1 = 2e^{-\left(\frac{4t}{L}\right)^2} \quad (9)$$

where the maximum number of iterations, denoted as  $L$ , while the current iteration is represented by  $t$ .

To update the position of the followers, Newton’s law of motion is employed, resulting in the following equation:

$$x_j^i = \frac{1}{2}at^2 + v_0t \quad (10)$$

where  $i \geq 2$ ,  $x_j^i$  represents the position of the  $i$ th follower salp in the  $j$ th dimension at time  $t$ . The initial speed is denoted by  $v_0$ , and we define  $a = \frac{v_{final}}{v_0}$ , where  $v = \frac{x-x_0}{t}$ . As the iteration represents the time in optimization, and 1 indicates the discrepancy between iterations, we consider the initial speed to be 0, leading to the following equation:

$$x_j^i = \frac{1}{2} (x_j^i + x_j^{i-1}) \quad (11)$$

The basic Pseudo-code of SSA is presented in Algorithm 1 [27].

**Remark 1.** We denote by  $T^*$ ,  $n^*$  and  $m^*$ , the optimized values of the FTSC parameters  $T$ ,  $n$  and  $m$ , respectively. Taking into account these notation, the proposed controller will developed in the next section.

## 4 Controller Design

The primary objective in managing the HBV transmission system is to decrease the counts of susceptible, acutely infected, and chronically infected individuals. As a result, through the proposed approach, our goal is to minimize the target state variables, specifically

$S$ ,  $I_1$ , and  $I_2$ , so that they approach their respective desired values represented as  $S_r$ ,  $I_{1r}$ , and  $I_{2r}$ . In this context, these desired values for each category are defined as  $S_r = I_{1r} = I_{2r} = 0$  [16], [42].

For the design of the proposed controller, we consider the following macrovariables:

$$\begin{cases} \psi_1 = S - S_r \\ \psi_2 = I_1 - I_{1r} \\ \psi_3 = I_2 - I_{2r}. \end{cases} \quad (12)$$

The evolution dynamic (6) can be developed and stated

as follows:

$$\begin{cases} \dot{\psi}_1 + T_1^* (\psi_1^{n^*/m^*} + \psi_1^{m^*/n^*}) = 0 \\ \dot{\psi}_2 + T_2^* (\psi_2^{n^*/m^*} + \psi_2^{m^*/n^*}) = 0 \\ \dot{\psi}_3 + T_3^* (\psi_3^{n^*/m^*} + \psi_3^{m^*/n^*}) = 0. \end{cases} \quad (13)$$

Calculating the time derivative of  $\psi_i|_{i=1,2,3}$ , substituting it with  $\dot{\psi}_i|_{i=1,2,3}$  in equation (13), rearranging and solve for  $u_1, u_2$  and  $u_3$  to get the control signals given by equation (14):

$$\begin{cases} u_1 = - \frac{\left(-T_2^* \left(I_1 - I_{1r}^{n^*/m^*} + I_1 - I_{1r}^{m^*/n^*}\right) + \dot{I}_{1r} - \alpha S I_2 + (\beta + \gamma_1 + \mu_0) I_1\right)}{\alpha S I_2} + \\ \frac{I_1 \left(-T_3^* \left(I_2 - I_{2r}^{n^*/m^*} + I_2 - I_{2r}^{m^*/n^*}\right) + \dot{I}_{2r} - \beta I_1 + (\gamma_2 + \mu_0 + \mu_1) I_2\right)}{\alpha S I_2^2} \\ u_2 = \frac{\left(-T_1^* \left((S - S_r)^{n^*/m^*} + (S - S_r)^{m^*/n^*}\right) + \dot{S}_r - b + S \mu_0\right)}{S} + \\ \frac{\left(-T_2^* \left((I_1 - I_{1r})^{n^*/m^*} + (I_1 - I_{1r})^{m^*/n^*}\right) + \dot{I}_{1r} + (\beta + \gamma_1 + \mu_0) I_1\right)}{S} - \\ \frac{(S + I_1) \left(-T_3^* \left(I_2 - I_{2r}^{n^*/m^*} + I_2 - I_{2r}^{m^*/n^*}\right) + \dot{I}_{2r} - \beta I_1 + (\gamma_2 + \mu_0 + \mu_1) I_2\right)}{S I_2} \\ u_3 = - \frac{\left(-T_1^* \left((S - S_r)^{n^*/m^*} + (S - S_r)^{m^*/n^*}\right) + \dot{S}_r - b + \alpha S I_2 + \mu_0 S\right)}{S} - \\ \frac{\left(-T_2^* \left((I_1 - I_{1r})^{n^*/m^*} + (I_1 - I_{1r})^{m^*/n^*}\right) + \dot{I}_{1r} - \alpha S I_2 + (\beta + \gamma_1 + \mu_0) I_1\right)}{S} + \\ \frac{\left(-T_3^* \left(I_2 - I_{2r}^{n^*/m^*} + I_2 - I_{2r}^{m^*/n^*}\right) + \dot{I}_{2r} - \beta I_1 + (\gamma_2 + \mu_0 + \mu_1) I_2\right) I_1}{S I_2}. \end{cases} \quad (14)$$

The proposed controller scheme is illustrated by the following scheme:

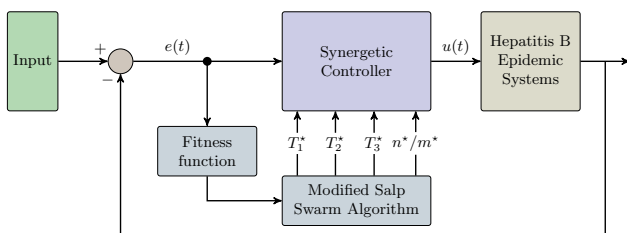


Figure 2: Closed-loop scheme of the proposed controller.

*Proof.* Consider the Lyapunov function  $V$ :

$$\begin{aligned} V &= \frac{1}{2} (\varphi_1^T \varphi_1 + \varphi_2^T \varphi_2 + \varphi_3^T \varphi_3) \\ &= \frac{1}{2} (\varphi_1^2 + \varphi_2^2 + \varphi_3^2) = v_1 + v_2 + v_3, \end{aligned} \quad (15)$$

where,

$$v_i = \frac{1}{2} \varphi_i^2, \quad \forall i \in \{1, 2, 3\}. \quad (16)$$

The time derivative of  $V$  is:

**Theorem 1.** *In the context of system (2), when the control input is defined as in equation (14), the designated aggregated macrovariables in equation (12) ultimately converge to the invariant manifold  $\varphi(x, t) = 0$  within a fixed-time.*

$$\begin{aligned}
\dot{V} &= \varphi_1 \dot{\varphi}_1 + \varphi_2 \dot{\varphi}_2 + \varphi_3 \dot{\varphi}_3 \\
&= -T_1^* \left( \varphi_1 \left( \varphi_1^{n^*/m^*} + \varphi_1^{(m^*/n^*)} \right) \right) - T_2^* \left( \varphi_2 \left( \varphi_2^{n^*/m^*} + \varphi_2^{(m^*/n^*)} \right) \right) - T_3^* \left( \varphi_3 \left( \varphi_3^{n^*/m^*} + \varphi_3^{(m^*/n^*)} \right) \right) \\
&= -T_1^* \left( \varphi_1^{\frac{n^*+m^*}{m^*}} + \varphi_1^{\frac{n^*+m^*}{n^*}} \right) - T_2^* \left( \varphi_2^{\frac{n^*+m^*}{m^*}} + \varphi_2^{\frac{n^*+m^*}{n^*}} \right) - T_3^* \left( \varphi_3^{\frac{n^*+m^*}{m^*}} + \varphi_3^{\frac{n^*+m^*}{n^*}} \right) \\
&= -T_1^* \left( (2v_1)^{\frac{n^*+m^*}{2}} + (2v_1)^{\frac{n^*+m^*}{2}} \right) - T_2^* \left( (2v_2)^{\frac{n^*+m^*}{2}} + (2v_2)^{\frac{n^*+m^*}{2}} \right) - T_3^* \left( (2v_3)^{\frac{n^*+m^*}{2}} + (2v_3)^{\frac{n^*+m^*}{2}} \right).
\end{aligned} \tag{17}$$

Therefore,  $\dot{V} \leq 0$  since  $m^* + n^*$  is even number. Thus, the control law defined by equation (14) guarantees the stability of the HBV transmission system.

Let's consider now that  $W = 2V$  and  $w_i = 2v_i$ , then (17) can be written as follows:

$$\begin{aligned}
\dot{W} &= -T_1^* \left( w_1^{\left( \frac{n^*+m^*}{2n^*} \right)} + w_1^{\left( \frac{n^*+m^*}{2m^*} \right)} \right) - T_2^* \left( w_2^{\left( \frac{m^*+n^*}{2n^*} \right)} + w_2^{\left( \frac{m^*+n^*}{2m^*} \right)} \right) - T_3^* \left( w_3^{\left( \frac{m^*+n^*}{2n^*} \right)} + w_3^{\left( \frac{m^*+n^*}{2m^*} \right)} \right) \\
&= -T_1^* (w_1^{\gamma_1} + w_1^{\gamma_2}) - T_2^* (w_2^{\gamma_1} + w_2^{\gamma_2}) - T_3^* (w_3^{\gamma_1} + w_3^{\gamma_2})
\end{aligned} \tag{18}$$

where  $\gamma_1 = \frac{n^*+m^*}{2n^*}$  and  $\gamma_2 = \frac{n^*+m^*}{2m^*}$ .

In order for the function  $\dot{W}$  to be negative definite, the values of  $n^* > 1$  and  $m^* > 1$ , in accordance to Lemma 1 must be odd numbers, therefore,  $1 < \gamma_1$  and  $0 < \gamma_2 < 1$ . Thus, the functions  $W$  and  $V$  within a fixed-time, they converge to zero, and forcing the macrovariable  $\varphi$  to reach the invariant manifold  $\varphi(x, t) = 0$ . The proof is completed.  $\square$

**Remark 2.** Without the optimization method, one can chose the values of  $n^* > 1$  and  $m^* > 1$  to be odd numbers, and thus the negative definiteness of  $\dot{W}$  is guaranteed. In contrast, in order for the Lyapunov function  $\dot{W}$  to exhibit negative definiteness in the case of optimisation, it is necessary for the optimised parameters  $n^*$  and  $m^*$  to be odd integers. To satisfy this requirement, we have incorporated additional conditions into the SSA algorithm to guarantee that the optimized values obtained are always odd. The structure of the proposed modified algorithm is shown in algorithm 2.

To address the concern mentioned in Remark 2, we propose an approach to approximate the fraction  $\frac{n}{m}$  with nearly exact precision. This involves projecting all the salps into the set of odd feasible numbers, denoted as  $\Omega_{\frac{n}{m}}$ , which is defined as follows:

$$\Omega_{\frac{n}{m}} = \left\{ p, q \in \mathbb{N}^* \mid (lb < \frac{p}{q} < ub) \wedge (pq \bmod 2 = 1) \right\}. \tag{19}$$

Thus,  $\frac{n^*}{m^*} = P_{\Omega_{\frac{n}{m}}}(\frac{n}{m})$ , with  $P_{\Omega_{\frac{n}{m}}}(\frac{n}{m})$  means the projection of  $\frac{n}{m}$  into the set  $\Omega_{\frac{n}{m}}$ .

In order to implement the above solution, we propose a Modified Salp Swarm Algorithm (MSSA) presented in Algorithm 2. The MSSA calculate the projection and perform the SSA optimization at the same time.

---

#### Algorithm 2 MSSA Pseudo-code.

---

- 1: Generate the salp populations  $x_i$  ( $i = 1, \dots, k_1$ ) according to  $lb$ ;
  - 2: **while** Stop condition is not satisfied **do**  $\triangleright$   
the fitness function error is negligible between two successive search agents ( $< \epsilon$ )
  - 3:     Calculate the fitness of each search agent "salp"
  - 4:      $\frac{n^*}{m^*}$  = the best search agent couple
  - 5:     Update  $c_1$  by Eq (9)
  - 6:     **for** each salp  $x_i$  **do**
  - 7:          $\frac{p_i}{q_j} \leftarrow rat(x_i)$   $\triangleright$  format rational in Matlab
  - 8:          $n_i \leftarrow p_i \times (10^A + 1) + 1 - p_i \bmod 2$   $\triangleright$   
You can substitute any large enough odd number instead of  $10^A + 1$
  - 9:          $m_j \leftarrow q_j \times (10^A + 1) + 1 - q_j \bmod 2$
  - 10:          $x_i \leftarrow \frac{n_i}{m_i}$
  - 11:         **if** ( $i = 1$ ) **then**
  - 12:             Adjust/Update the position of the leading salp by Eq (8)
  - 13:         **else**
  - 14:             Adjust/Update the position of the leading salp by Eq (11)
  - 15:         **end if**
  - 16:     **end for**
  - 17:     Based on the upper and lower boundaries of the variables, amend the salps
  - 18: **end while**
  - 19: return  $n^*, m^*$
- 

The accuracy parameter  $A$  in Algorithm 2 enables us to control the accuracy of the projection's approximation according to the following theorem:

**Theorem 2.** *As the value of  $A$  increases, the error diminishes, resulting in a closer projection and a higher level of accuracy in the approximation.*

*Proof.* We suppose that

$$\frac{m}{n} = rat\left(\frac{m}{n}\right) = \frac{p}{q}. \tag{20}$$

Thus,

$$\begin{aligned}
 e_A &= \left| \frac{m}{n} - \frac{p \times (10^A + 1) + 1 - p \pmod 2}{q \times (10^A + 1) - q \pmod 2} \right| \\
 &= \left| \frac{p}{q} - \frac{p \times (10^A + 1) + 1 - p \pmod 2}{q \times (10^A + 1) + 1 - q \pmod 2} \right| \quad (21) \\
 &= \left| \frac{p + q - p(q \pmod 2) + q(p \pmod 2)}{q^2 \times (10^A + 1) + q + q(q \pmod 2)} \right|
 \end{aligned}$$

Similarly,

$$\begin{aligned}
 e_{A+1} &= \left| \frac{p}{q} - \frac{p \times (10^{A+1} + 1) + 1 - p \pmod 2}{q \times (10^{A+1} + 1) + 1 - q \pmod 2} \right| \quad (22) \\
 &= \left| \frac{p + q - p(q \pmod 2) + q(p \pmod 2)}{q^2 \times (10^{A+1} + 1) + q + q(q \pmod 2)} \right|
 \end{aligned}$$

It is evident that when  $p$  is an odd number,  $q$  is an even, and vice versa. Therefore, the expression  $q(p \pmod 2) - p(q \pmod 2)$  can never equal 0. Additionally, both  $p$  and  $q$  are non-null integer numbers, thereby enforcing strict inequality.

Thus,  $e_{A+1} < e_A, \forall \text{ integer } A \gg 0$ . As the magnitude of  $A$  increases, the error diminishes, leading to a closer projection and a more accurate approximation. This fulfills the requirements for the proof.  $\square$

## 5 Simulation Results and Discussion

The mathematical model, along with the control variables presented in equation (14), has been implemented using the Matlab Simulink framework. The simulation incorporates the following parameters:  $b = 0.0121$ ,  $\alpha = 0.8$ ,  $\mu_0 = 0.0121$ ,  $\beta = 0.025$ ,  $\gamma_1 = 0.05$ ,  $\gamma_2 = 0.5$ ,  $\mu_1 = 0.02$ , and  $v = 0.02$ . Based on [15], we can consider the initial conditions of the system as:  $S(0) = 100$ ,  $I_1(0) = 20$ ,  $I_2(0) = 20$  and  $R(0) = 12$ . During the simulation, the time responses of the control system were solved using the Runge-Kutta fourth order method. The simulation time spanned from  $t = 0$  to  $t = 10$  days, with an incremental time step of 0.01 day. The obtained results are shown in figures 3-7.

In Figure 3, we observe the epidemic transmission dynamics in the absence of any control intervention. Despite the passage of 30 days, the disease remains prevalent and the transmission from susceptible individuals to those with acute and chronic infections persists. Notably, at the 30-day mark, the population of individuals with acute disease, denoted by  $I_1$ , exceeds 10%, a value significantly higher than the stabilization threshold. These findings suggest that without effective interventions, the disease may continue to spread and pose a significant public health threat. Further investigation and implementation of control measures are warranted to mitigate the impact of the epidemic.

In Figure 4, we present a comparison between two control methods applied to the system given by equation 2 without any optimization setup: SC and FTSC controllers. The control equations and the convergence theorem of FTSC are detailed in Section 4. Through the comparison, we observe that FTSC yields superior

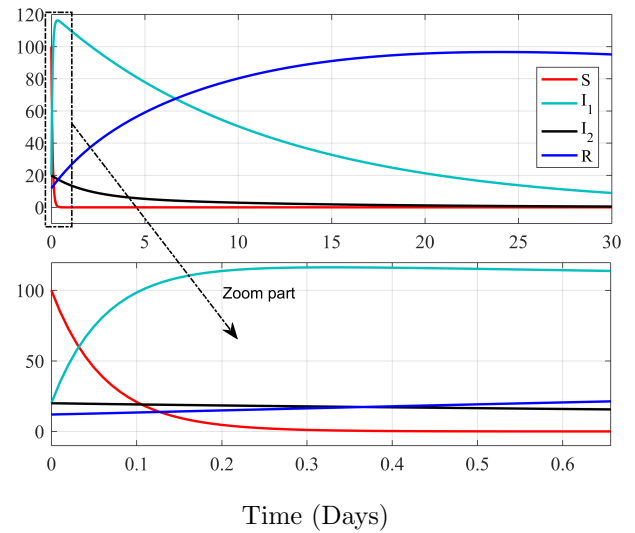


Figure 3: Disease behavior without control.

control performance compared to SC, with a faster convergence rate and lower steady-state error. These results support the effectiveness of FTSC in controlling the considered system.

In our study, we carefully selected the values for the gains of the FTSC, denoted by  $T_1, T_2, T_3, n$ , and  $m$ . Conversely, we used the same values of  $T_1, T_2, T_3$  for the SC method. The use of the same gains in SC allows for a direct comparison with FTSC, with the only difference being the control methodology employed. By randomly generating the gains of FTSC, we aimed to explore the effectiveness of the method under various scenarios and gain configurations. These results contribute to the understanding of the robustness and adaptability of FTSC for control applications.

We observe that the considered system stabilizes after 5 days, outperforming the system presented in figure 3. In terms of the comparison between SC and FTSC, we note that SC performs comparably to FTSC for infected individuals with chronic disease and recovered individuals (as shown in subfigures figure 4.c and figure 4.d). However, in subfigure figure 4.a, we observe that FTSC achieves stabilization one day earlier than SC, indicating its superior control performance in this case. These findings suggest that FTSC may be particularly effective in such scenarios.

Furthermore, we observe that instability occurs in the SC method for the population of individuals with acute infection, as demonstrated in figure 4.b. Despite this, both controllers have demonstrated effective stabilization of the system overall. The observed instability in SC highlights the potential limitations of this method in controlling systems with complex dynamics. These findings suggest that alternative control methodologies, such as FTSC, may provide more robust and effective control in such scenarios.

Figure 5 illustrates the signal control of the three parameters (Vaccination, Isolation, Treatment) without employing an optimization algorithm. It is evident

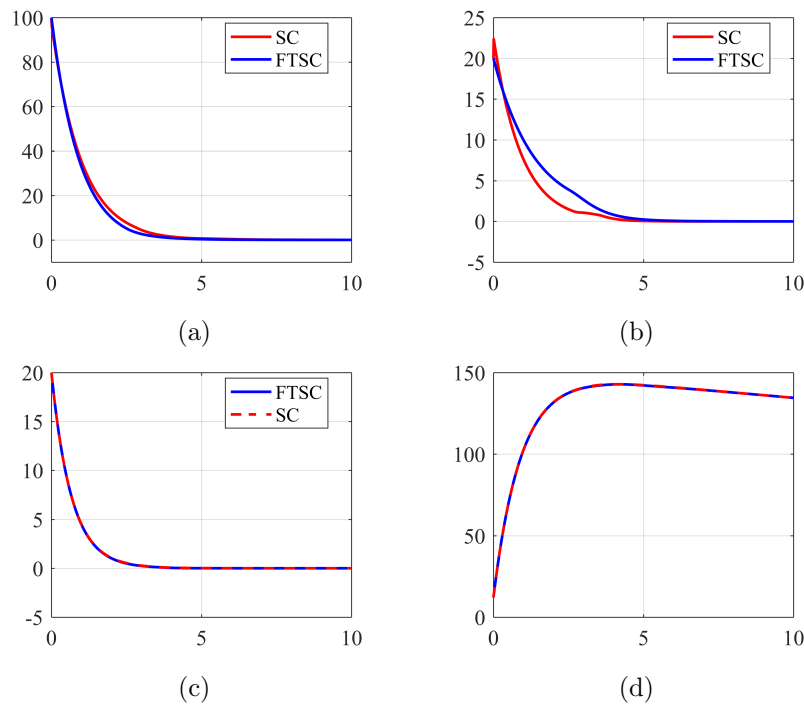


Figure 4: The behavior of HVB under FTSC and SC without optimization algorithm; (a), (b), (c) and (d) successively presents the susceptible, acute infected, chronic infected individuals, and the recovered ones with life-time immunity.

that the FTSC utilizes more resources compared to the SC. In fact, FTSC fully exhausts the available vaccination power, whereas SC utilizes only a small portion of it.

To demonstrate the superior performance of FTSC, we introduce the Salp Swarm optimization Algorithm to both controllers. Figure 6 showcases the outcomes of this protocol, clearly indicating the distinct advantage of FTSC. The Optimized FTSC (OFTSC) achieves stabilization in less than 2.5 days for both acute and chronic infected individuals. On the other hand, the Optimized SC (OSC) requires approximately 4 days to stabilize acute infected individuals and more than 3 days for chronic infected individuals. The remaining curves exhibit similar results across the two controllers.

Based on the analysis presented in figure 6, it can be inferred that the recovery time between the OFTSC and OSC controllers is relatively similar. However, a notable distinction arises in terms of the duration for which individuals remain afflicted by illness. By employing the OFTSC controller, the period of sickness is significantly reduced, accounting for approximately 30% of the total convergence time.

Analyzing the control signals depicted in figure 7, it is evident that both OFTSC and OSC have fixed values of 1 for the isolation and vaccination signals, representing the maximum possible levels of these interventions. However, the key difference lies in the treatment control signal, which is set to 0 for OSC and 1 for OFTSC. This discrepancy indicates that OFTSC effectively utilizes the available power of isolation, vaccination, and

treatment to a greater extent compared to OSC.

In conclusion, after incorporating the SSA into both controllers, favorable results have been achieved. However, a clear superiority of 30% is observed in favor of OFTSC. This outcome provides strong evidence for the effectiveness of FTSC and highlights the positive impact of SSA on both controllers. The findings demonstrate the potential of FTSC as an efficient control strategy and emphasize the value of leveraging SSA to enhance control performance in similar systems.

## 6 Conclusion

In conclusion, this research paper presents a novel approach for combating hepatitis B infection through an SSA optimized fixed-time synergetic control strategy. By leveraging an enhanced version of the SSA algorithm, the optimization challenge posed by fractional power restrictions is effectively addressed. The proposed strategy focuses on minimizing the prevalence of susceptible, acute infected, and chronically infected individuals by employing control variables such as isolation, treatment, and vaccination. Through numerical simulations, it has been demonstrated that the fixed-time synergetic control approach, especially when optimized, outperforms the conventional synergetic control method. The significant reduction in total convergence time achieved by the FTSC strategy highlights its potential for effectively controlling and managing the spread of hepatitis B infection. This research contributes to the growing body of knowledge on epidemic control strategies and underscores the impor-

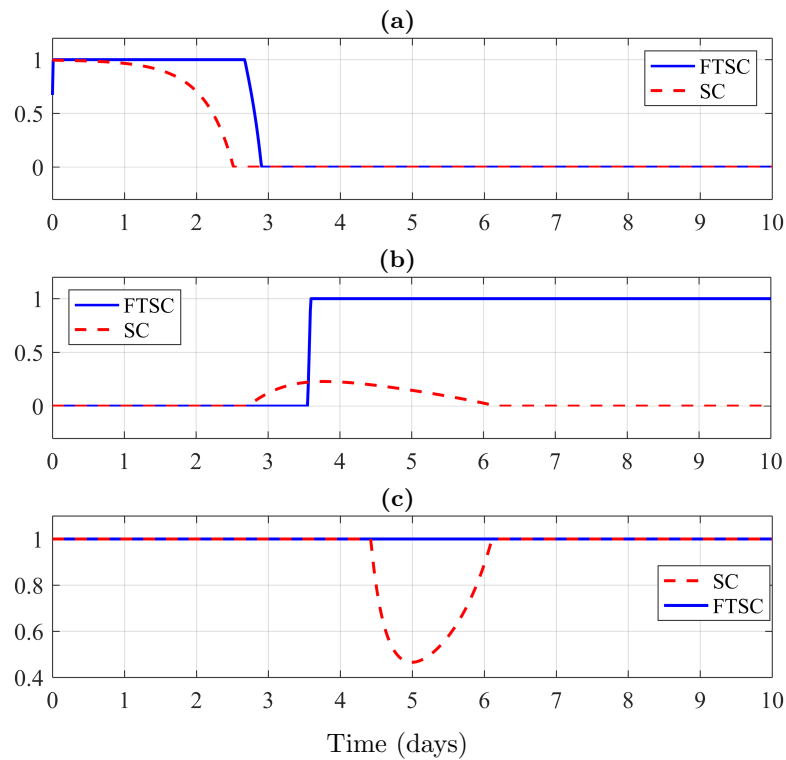


Figure 5: The control signal of FTSC and SC inputs without optimization : (a) isolation, (b) treatment, and (c) vaccination.

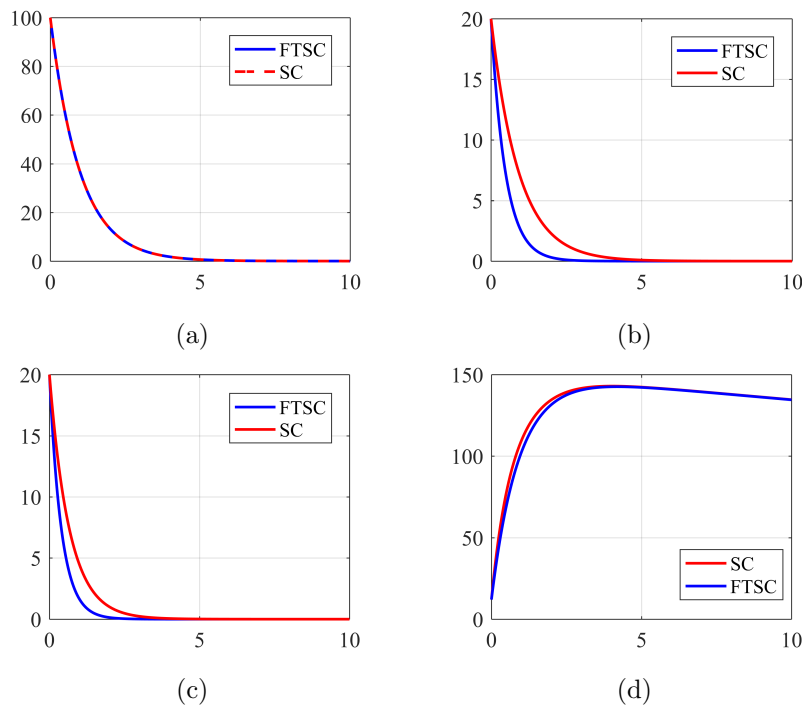


Figure 6: The behavior of HVB under FTSC and SC with SSA optimization, where (a), (b), (c) and (d) are successively presents the susceptible, acute infected, chronic infected individuals, and the recovered ones with life-time immunity.

tance of optimization techniques in achieving improved outcomes. Further studies and real-world applications of the proposed approach hold promise for enhancing public health efforts and mitigating the impact of hepatitis B infections worldwide.

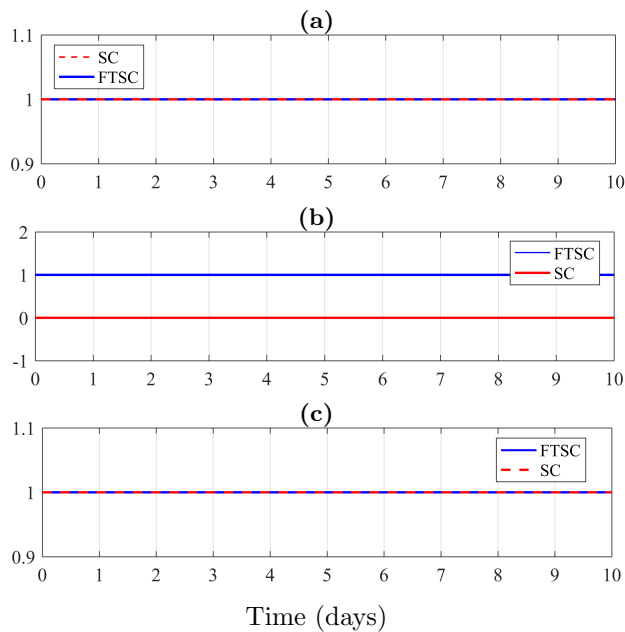


Figure 7: The control signal of FTSC and SC inputs with SSA optimization algorithm: (a) isolation, (b) treatment, and (c) vaccination.

## References

- [1] ABUSNAINA, A. A., AHMAD, S., JARRAR, R., AND MAFARJA, M. Training neural networks using salp swarm algorithm for pattern classification. In *Proceedings of the 2nd international conference on future networks and distributed systems* (2018), pp. 1–6.
- [2] AL-HUSSEIN, A.-B. A., TAHIR, F. R., AND PHAM, V.-T. Fixed-time synergetic control for chaos suppression in endocrine glucose–insulin regulatory system. *Control Engineering Practice* 108 (2021), 104723.
- [3] AL-SADEQ, D. W., TALEB, S. A., ZAIED, R. E., FAHAD, S. M., SMATTI, M. K., RIZEQ, B. R., AL THANI, A. A., YASSINE, H. M., AND NASRALLAH, G. K. Hepatitis b virus molecular epidemiology, host-virus interaction, coinfection, and laboratory diagnosis in the mena region: An update. *Pathogens* 8, 2 (2019), 63.
- [4] ALTER, M. J., EVATT, B. L., MARGOLIS, H. S., BISWAS, R., EPSTEIN, J. S., FEINSTONE, S. M., FINLAYSON, J. S., TANKERSLEY, D., ALTER, H. J., AND HOOFNAGEL, J. H. Public health service interagency guidelines for screening donors of blood, plasma, organs, tissues, and semen for evidence of hepatitis b and hepatitis c. *American Journal of Infection Control* 19, 5 (1991), 32A–41A.
- [5] BOONYAPRAPASORN, A., CHOOPJCHAROEN, T., PENGWANG, E., MANEEWARN, T., NATSUPAKPONG, S., SA-NGIAMSUNTHORN, P., SUECHOEI, A., AND WECHSATHOL, W. Control of ebola epidemic system based on terminal synergetic controller design. In *2019 IEEE International Conference on Automatic Control and Intelligent Systems (I2CACIS)* (2019), IEEE, pp. 204–209.
- [6] BOONYAPRAPASORN, A., NATSUPAKPONG, S., NGIAMSUNTHORN, P. S., AND THUNG-OD, K. An application of finite time synergetic control for vaccination in epidemic systems. In *2017 IEEE Conference on Systems, Process and Control (IC-SPC)* (2017), IEEE, pp. 30–35.
- [7] CAMACHO-VILLALÓN, C. L., DORIGO, M., AND STÜTZLE, T. An analysis of why cuckoo search does not bring any novel ideas to optimization. *Computers & Operations Research* 142 (2022), 105747.
- [8] CAMACHO-VILLALÓN, C. L., DORIGO, M., AND STÜTZLE, T. Exposing the grey wolf, moth-flame, whale, firefly, bat, and antlion algorithms: six misleading optimization techniques inspired by bestial metaphors. *International Transactions in Operational Research* 30, 6 (2023), 2945–2971.
- [9] CASTELLI, M., MANZONI, L., MARIOT, L., NOBILE, M. S., AND TANGHERLONI, A. Salp swarm optimization: a critical review. *Expert Systems with Applications* 189 (2022), 116029.
- [10] DONTWI, I., OBENG-DENTEH, W., OBIRI-APRAKU, L., AND ANDAM, E. Modelling hepatitis b in a high prevalence district in ghana.
- [11] HUANG, S., XIONG, L., WANG, J., LI, P., WANG, Z., AND MA, M. Fixed-time synergetic controller for stabilization of hydraulic turbine regulating system. *Renewable Energy* 157 (2020), 1233–1242.
- [12] KAMYAD, A. V., AKBARI, R., HEYDARI, A. A., HEYDARI, A., ET AL. Mathematical modeling of transmission dynamics and optimal control of vaccination and treatment for hepatitis b virus. *Computational and mathematical methods in medicine* 2014 (2014).
- [13] KANAGARAJ, G., MASTHAN, S. S., AND VINCENT, F. Y. Meta-heuristics based inverse kinematics of robot manipulator’s path tracking capability under joint limits. In *Mendel* (2022), vol. 28, pp. 41–54.
- [14] KANCHANAHARUTHAI, A. Nonlinear controller design for hydraulic turbine regulating systems via immersion and invariance. *International Journal of Control* (2023), 1–15.
- [15] KHAN, T., ZAMAN, G., AND ALGAHTANI, O. Transmission dynamic and vaccination of hepatitis b epidemic model. *WULFENIA J* 22, 2 (2015), 230–241.
- [16] KHAN, T., ZAMAN, G., AND CHOCHAN, M. I. The transmission dynamic and optimal control of acute and chronic hepatitis b. *Journal of biological dynamics* 11, 1 (2017), 172–189.
- [17] KHEIREDDINE, C., YASSINE, A., FAWZI, S., AND KHALIL, M. A robust synergetic controller for quadrotor obstacle avoidance using bézier curve versus b-spline trajectory generation. *Intelligent Service Robotics* 15, 1 (2022), 143–152.

- [18] KIM, G., AND KIM, A. Scan context: Egocentric spatial descriptor for place recognition within 3d point cloud map. In *2018 IEEE/RSJ International Conference on Intelligent Robots and Systems (IROS)* (2018), IEEE, pp. 4802–4809.
- [19] KOLESNIKOV, A. A. Introduction of synergetic control. In *2014 American control conference* (2014), IEEE, pp. 3013–3016.
- [20] KONDRATIEV, I., SANTI, E., AND DOUGAL, R. Robust nonlinear synergetic control for m-parallel-connected dc-dc boost converters. In *2008 IEEE power electronics specialists conference* (2008), IEEE, pp. 2222–2228.
- [21] KRUPOVIC, M., BLOMBERG, J., COFFIN, J. M., DASGUPTA, I., FAN, H., GEERING, A. D., GIFFORD, R., HARRACH, B., HULL, R., JOHNSON, W., ET AL. Ortervirales: new virus order unifying five families of reverse-transcribing viruses. *Journal of virology* 92, 12 (2018), 10–1128.
- [22] KUDELA, J. A critical problem in benchmarking and analysis of evolutionary computation methods. *Nature Machine Intelligence* 4, 12 (2022), 1238–1245.
- [23] LI, D., XI, W., ZHANG, Z., REN, L., DENG, C., CHEN, J., SUN, C., ZHANG, N., AND XU, J. Oral microbial community analysis of the patients in the progression of liver cancer. *Microbial Pathogenesis* 149 (2020), 104479.
- [24] LU, S., TIAN, C., AND YAN, P. Adaptive extended state observer-based synergetic control for a long-stroke compliant microstage with stress stiffening. *IEEE/ASME Transactions on Mechatronics* 25, 1 (2019), 259–270.
- [25] MAGNIUS, L., MASON, W. S., TAYLOR, J., KANN, M., GLEBE, D., DÉNY, P., SUREAU, C., NORDER, H., AND CONSORTIUM, I. R. Ictv virus taxonomy profile: Hepadnaviridae. *Journal of General Virology* 101, 6 (2020), 571–572.
- [26] MERTA, J., AND BRANDEJSKÝ, T. Three-dimensional genetic algorithm for the kirkman’s schoolgirl problem. In *Mendel* (2018), Vysoké učení technické v Brně.
- [27] MIRJALILI, S., GANDOMI, A. H., MIRJALILI, S. Z., SAREMI, S., FARIS, H., AND MIRJALILI, S. M. Salp swarm algorithm: A bio-inspired optimizer for engineering design problems. *Advances in engineering software* 114 (2017), 163–191.
- [28] NANA-KYERE, S., ACKORA-PRAH, J., OKYERE, E., MARMAN, S., AND AFRAM, T. Hepatitis b optimal control model with vertical transmission. *Appl. Math* 7, 1 (2017), 5–13.
- [29] NUSAWARDHANA, ZAK, S., AND CROSSLEY, W. Nonlinear synergetic optimal controllers. *Journal of guidance, control, and dynamics* 30, 4 (2007), 1134–1147.
- [30] OUSSAMA, M., ABDELGHANI, C., AND LAKHDAR, C. Efficiency and robustness of type-2 fractional fuzzy pid design using salps swarm algorithm for a wind turbine control under uncertainty. *ISA transactions* 125 (2022), 72–84.
- [31] SANTI, E., MONTI, A., LI, D., PRODDUTUR, K., AND DOUGAL, R. Synergetic control for power electronics applications: A comparison with the sliding mode approach. *Journal of Circuits, Systems, and Computers* 13, 04 (2004), 737–760.
- [32] SAYINER, M., GOLABI, P., AND YOUNOSSE, Z. M. Disease burden of hepatocellular carcinoma: a global perspective. *Digestive diseases and sciences* 64 (2019), 910–917.
- [33] SHARIFI, A., AND SALARIEH, H. An adaptive synergetic controller applied to heavy-duty gas turbine unit. *Applied Energy* 333 (2023), 120535.
- [34] SOLANKI, P., AND DEEP, K. Quadratic approximation salp swarm algorithm for function optimization. *OPSEARCH* (2023), 1–33.
- [35] SUN, Y., DEMAGNY, H., FAURE, A., PONTANARI, F., JALIL, A., BRESCIANI, N., YILDIZ, E., KORBELIUS, M., PERINO, A., SCHOONJANS, K., ET AL. Asparagine protects pericentral hepatocytes during acute liver injury. *The Journal of Clinical Investigation* 133, 7 (2023).
- [36] VESELOV, G. E., SKLYAROV, A. A., AND SKLYAROV, S. A. Synergetic approach to quadrotor helicopter control with attractor-repeller strategy of nondeterministic obstacles avoidance. In *2014 6th International Congress on Ultra Modern Telecommunications and Control Systems and Workshops (ICUMT)* (2014), IEEE, pp. 228–235.
- [37] WANG, J., PANG, J., AND LIU, X. Modelling diseases with relapse and nonlinear incidence of infection: a multi-group epidemic model. *Journal of biological dynamics* 8, 1 (2014), 99–116.
- [38] WANG, J., ZHANG, R., AND KUNIYA, T. The stability analysis of an sveir model with continuous age-structure in the exposed and infectious classes. *Journal of biological dynamics* 9, 1 (2015), 73–101.
- [39] WILLIAMS, R. Global challenges in liver disease. *Hepatology* 44, 3 (2006), 521–526.
- [40] ZAMAN, G., KANG, Y. H., AND JUNG, I. H. Stability analysis and optimal vaccination of an sir epidemic model. *BioSystems* 93, 3 (2008), 240–249.
- [41] ZAMAN, G., KANG, Y. H., AND JUNG, I. H. Optimal treatment of an sir epidemic model with time delay. *BioSystems* 98, 1 (2009), 43–50.
- [42] ZIOUI, N., TADJINE, M., AND BOUCHERIT, M. S. Super-twisting algorithm approach to control tumors growth. In *3rd International Conference on Systems and Control* (2013), IEEE, pp. 457–461.